

# Evaluation of Microbiological Corrosion of API 5L X80 Steel by Electrochemical Techniques in Produced Water by the Oil Industry

Edkarlla Sousa Dantas de Oliveira<sup>a\*</sup>, Roseana Florentino da Costa Pereira<sup>a</sup>, Maria Alice Gomes

de Andrade Lima<sup>b</sup>, Severino Leopoldino Urtiga Filho<sup>a</sup>

<sup>a</sup>Universidade Federal de Pernambuco, Departamento de Engenharia Mecânica, Av. Prof. Moraes Rego, 1235, Cidade Universitária, 50670-901, Recife, PE, Brasil

<sup>b</sup>Universidade Federal de Pernambuco, Departamento de Engenharia Química, Av. Prof. Arthur Sá s/n, Cidade Universitária, 50740-521, Recife, PE, Brasil

Received: September 17, 2019; Accepted: March 16, 2020

Corrosion of pipelines can be significantly affected by the activity of microorganisms present in the environment. The objective of this work was to investigate the influence microbial in the corrosion behavior of API 5L X80 steel in produced water by open circuit potential, polarization curves and electrochemical impedance spectroscopy measurements. Physical-chemical and microbiological analyzes were performed in the produced water and the tests were conducted in biotic and abiotic systems. The films and corrosion morphology developed in the steel over time were characterized by scanning electron microscopy. The results confirm that the activity of the consortium of microorganisms in the formed biofilm accelerated the dissolution of the iron, causing pitting corrosion in the steel exposed to the biotic system. Through the adjustment of the equivalent electrochemical circuit, the impedance results allowed to interpret the interactions between electrode, film and electrolyte.

**Keywords:** API 5L X80 steel, electrochemical techniques, microbiological corrosion, produced water.

## 1. Introduction

A common problem in the oil industry is the corrosion of carbon steel pipeline by produced water. The produced water is the largest residue generated during the exploration and drilling of oil and natural gas wells<sup>1,2</sup>. This effluent presents high salinity, suspended and dissolved solids, residual hydrocarbons, organic species, metals, radioactive compounds and a great diversity of microbial species, particularly of bacteria<sup>3,4</sup>. Bacteria are generally more studied due to their involvement in biofilm formation through the interaction of the bacterial consortium and because they also facilitate the growth of different types of microorganisms<sup>5</sup>. In general, the biological activity of microorganisms (oxidation and reduction of some elements, corrosive acid production and depolarization of the corrosion cell) within biofilms causes microbiologically induced corrosion (MIC), more specifically localized corrosion (pitting corrosion) of pipelines<sup>6</sup>. In addition, the interfacial behavior of the metals in the electrolyte is modified, due to changes in ion concentration, pH value and oxidation-reduction potential induced by biofilm formation<sup>7</sup>. AlAbbas et al. have recently published a paper using electrochemical tests in the study of the effect of sulfate-reducing bacteria (SRB) on the corrosion

behavior of API 5L X80 steel<sup>8</sup>. The results showed that SRB increased pitting corrosion in steel due to biofilm formation and the production of porous iron sulphide. Misha evaluated by electrochemical techniques the activity of iron-reducing bacteria in the corrosion of API 5L X80 steel<sup>9</sup>. The formation of the bacteria-stable biofilm decreased the corrosion of the steel due to limitations of mass transfer, whereas in the sterile system a mixed layer was formed, which favored the dissolution of the iron, increasing corrosion. Liu et al. investigated by electrochemical impedance, open circuit potential and polarization curve tests, the effect of iron oxidizing bacteria on the corrosion of Q235 carbon steel in produced water<sup>10</sup>. The researchers reported that the integrity of the formed biofilm was modified over time. With the maturation, there was the detachment of parts of the biofilm, due to the high metabolic activity of the bacteria, which accentuated the corrosion in the coupons. API 5L X80 steel has been investigated and characterized in systems containing isolated SRB cultures<sup>11-13</sup>. However, there are few studies correlating the effect of MIC on API 5L X80 steel in the presence of mixed consortia of microorganisms under static conditions. The objective of this work is to investigate the microbiological corrosion of API 5L X80 steel in produced water (abiotic and biotic systems) through electrochemical

\*e-mail: edkarllaquimica@hotmail.com

tests, and to correlate it with the behavior obtained in 3.5 wt% NaCl solution. The material was characterized by chemical composition analysis. The physicochemical and microbiological composition of the produced water was quantitatively characterized. Microscopic surface studies were used to support the results.

## 2. Experimental Procedure

### 2.1 Metal sample preparation

API 5L X80 steel coupons with the following chemical composition (%) were used: 0.08 C, 0.3 Si, 1.82 Mn, 0.009 P, 0.001 S, 0.17 Cr, 0.01 Ni, 0.20 Mo, 0.01 Cu, 0.037 Al, 0.024 V, 0.003 W, 0.021 Ti, 0.081 Nb and Fe balance. The analysis of the chemical composition of X80 steel was performed by optical emission spectrometry on ARL Metal Analyzer model 3460-MA-090 equipment. The coupons were machined with the dimensions of 10 x 10 x 5 mm; afterwards a copper wire was soldered to establish the electrical connection. Subsequently, they were embedded in a polyvinyl chloride mold (PVC) with non-conductive acrylic resin, presenting an exposed area of 100 mm<sup>2</sup>. After this step, they were abraded with sandpapers (# 220-1200) and polished with (3 and 1) μm diamond paste, washed with distilled water and degreased in isopropyl alcohol and acetone. Finally, the coupons were sterilized in ultraviolet light for 30 minutes before being inserted into the electrolyte, at 25 °C.

### 2.2 Electrolytes and microorganisms

The tests were performed with 3.5 wt% NaCl solution and produced water from the extraction of petroleum from onshore wells. Samples of produced water (10 L) were collected in a sterile flask and immediately analyzed for the physico-chemical parameters described in Table 1, according to the Standard Methods for the Examination of Water and Wastewater<sup>14</sup>. As the present work is part of a series of studies, the major groups of microorganisms associated with microbiologically induced corrosion has already been published and is presented in Table 2<sup>15</sup>.

**Table 1.** Physical-chemical parameters of produced water.

Parameters	pH	SO <sub>4</sub> <sup>2-</sup> (mg/L)	S <sup>2-</sup> (mg/L)	NO <sub>3</sub> <sup>-</sup> (mg/L)	Cl <sup>-</sup> (mg/L)	Salinity (mg/L)	Fe (mg/L)	Oil and grease (mg/L)	TDS <sup>(a)</sup> (mg/L)	TSS <sup>(b)</sup> (mg/L)
Results	6.8	230.0	0.6	0.4	56.2	88.7	5.7	79.0	76.8	239.0

<sup>(a)</sup>Total Dissolved Solids; <sup>(b)</sup>Total Suspended Solids

**Table 2.** Microorganisms in the produced water<sup>15</sup>.

Groups of microorganisms	Total aerobic	Total anaerobic	Acid-producing aerobic	Acid-producing anaerobic	Precipitating iron bacteria	Sulfate-reducing bacteria
Cell concentration	1.2 x 10 <sup>4</sup> (CFU/mL)	1.1 x 10 <sup>3</sup> (MPN/mL)	7.0 x 10 (MPN/mL)	2.5 x 10 <sup>2</sup> (MPN/mL)	Undetected	4.5 x 10 <sup>3</sup> (MPN/mL)

### 2.3 Microorganisms culture

For the microbiological quantification, it was inoculated 1 mL of the produced water in reducing solutions, and subsequently reinoculated in the culture medium containing 30 g/L NaCl in 1 L of distilled water. The composition in (g/L) of the total aerobic bacteria culture medium was: 22.5 plate count agar (PCA) (pH 7.0). The composition in (g/L) of the total anaerobic bacteria culture medium prepared under nitrogen purge was as follows: 30.0 fluid medium to thioglycolate (pH 7.0). The composition in (g/L) of the acid-producing aerobic and anaerobic bacteria culture medium was: 10.0 sucrose, 10.0 tryptone, 1.0 beef extract and 0.018 phenol red (pH 7.2). Subsequently, the acid-producing anaerobic bacteria culture medium was purged with nitrogen. The composition in (g/L) of the SRB culture medium prepared under nitrogen purge was as follows: 0.5 KH<sub>2</sub>PO<sub>4</sub>, 1.0 NH<sub>4</sub>Cl, 1.0 Na<sub>2</sub>SO<sub>4</sub>, 0.67 CaCl<sub>2</sub>·2H<sub>2</sub>O, 1.68 MgCl<sub>2</sub>·6H<sub>2</sub>O, 7.0 mL sodium lactate (50%), 1.0 yeast extract, 0.1 ascorbic acid, 1.9 agar-agar, 4.0 mL resazurin (0.025%) and 0.5 FeSO<sub>4</sub>·7H<sub>2</sub>O (pH 7.6)<sup>16</sup>. The composition in (g/L) of the precipitating iron bacteria culture medium was: 30.0 NaCl, 0.5 (NH<sub>4</sub>)<sub>2</sub>SO<sub>4</sub>, 0.2 CaCl<sub>2</sub>·2H<sub>2</sub>O, 0.5 MgSO<sub>4</sub>·7H<sub>2</sub>O, 0.5 NaNO<sub>3</sub>, 10.0 ferric ammonium citrate and 0.5 K<sub>2</sub>HPO<sub>4</sub> (pH 7.0)<sup>17</sup>. The reducing solutions used were constituted in (g/L): 0.124 sodium thioglycolate, 0.1 ascorbic acid and 4.0 mL resazurin solution (0.025%) (pH 7.6). All groups of microorganisms were incubated at 35 °C. The culture medium and the reducing solutions were autoclaved at 1 atm, 121 °C for 15 minutes.

### 2.4 Electrochemical techniques

The electrochemical tests of open circuit potential (OCP), polarization curve (PC) and electrochemical impedance spectroscopy (EIS) were performed using a conventional three-electrode cell with the API 5L X80 steel coupons as working electrode, a saturated Ag/AgCl as reference and a platinum electrode as an auxiliary. The electrochemical measurements were performed on the AUTOLAB PGSTAT 100N<sup>®</sup> potentiostat coupled to a computer using NOVA 1.11

software. OCP and PC measurements were performed over 24 hours and after 24 hours, respectively. After the OCP assays, the polarization curves were performed starting from cathodic to anodic values, in the range between -0.4 V and +0.4 V vs Ag/AgCl, in relation to the corrosion potential ( $E_{\text{corr}}$ ), with a scan rate of  $3.3 \times 10^{-4}$  V/s. EIS measurements were performed after the following immersion times: 24, 48, 72, 192, 360, 720, 1080 and 1440 hours. The frequency rate applied was from  $10^5$  Hz to  $10^{-2}$  Hz and the potential perturbation amplitude of  $\pm 10$  mV. All electrochemical measurements were performed in triplicate, 25 °C and atmosphere without aeration. Three systems were used in the experiments. The 3.5 wt% NaCl solution (system) was used to observe the behavior of API 5L X80 steel in a conductive medium with salinity equivalent to seawater salinity (approximately 35 g/L). The abiotic system was established after the filtration of the produced water in sterile membranes with a porosity of 0.22  $\mu\text{m}$ , followed by the addition of 1 mg/L of sodium hypochlorite. The biotic system was composed of produced water (without any additional treatment).

### 2.5 Surface analysis by scanning electron microscopy

After 360 hours, the coupons with film or biofilm were removed from the systems and immersed in 5% glutaraldehyde solution in sodium cacodylate buffer (0.1 M) for 24 hours. Subsequently, washes were performed in 0.1 M sodium cacodylate for 30 minutes to fix the films formed on the surface and dehydrated in acetone at concentrations between 30% and 100%. After this step, the coupons were metalized with gold and examined on the scanning electron microscope TESCAN MIRA 3, at 10 kV. For analysis of corrosion morphology, the films formed on the surface of the coupons were removed with a non-metallic spatula, then immersed in Clark solution, followed by ultrasonic cleaning. The coupons were cleaned in isopropyl alcohol and acetone, dried and weighed as described in ASTM G1-03 and examined in the SEM HITACHI TM 3000<sup>18</sup>.

## 3. Results and Discussion

### 3.1 Results of open circuit potential test

Figure 1 shows the potential variation ( $E$ ) vs time (s) of 3.5 wt% NaCl, abiotic and biotic systems over 24 hours.

Figure 1 shows the following increasing order of API 5L X80 steel at zero time: 3.5 wt% NaCl (-0.572 V vs Ag/AgCl) > biotic (-0.662 V vs Ag/AgCl) > abiotic (-0.645 V vs Ag/AgCl) indicating that the steel showed a more active behavior in the systems of produced water. This difference can be attributed to the more complex composition of the water produced, since presence of salts mainly of sulphate and chloride ions (Table 1) can accelerate the corrosion of steel<sup>19</sup>. The high concentration of chloride ions in the 3.5

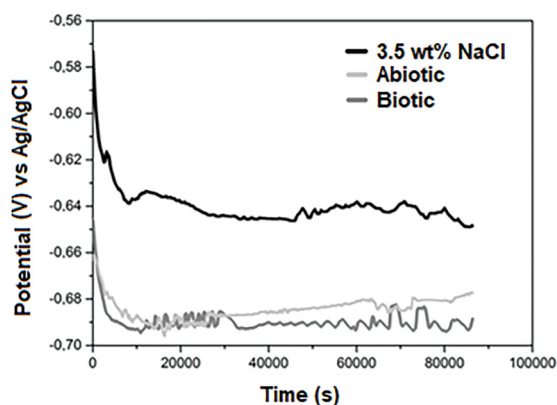


**Figure 1.** Variation of the open circuit potential in the 3.5 wt% NaCl, abiotic and biotic systems.

wt% NaCl system attacks the steel generating a large amount of corrosion products, which may be acting as a barrier to the electrolyte. Between 20000 seconds and 80000 seconds, potentials tend to stabilize, presenting a less negative value in the 3.5 wt% NaCl system, probably due to surface coverage by iron oxide. From 30000 seconds there was a small distinction in the values of the potentials evidencing the more negative potential for the biotic system. A quick analysis of these results could indicate greater susceptibility to corrosion of API 5L X80 steel in the biotic system. However, considering the differences between systems such as salinity and pH, other phenomena could be occurring on the surface of API 5L X80 steel which can't be detected by corrosion potential monitoring. Therefore, electrochemical analyses of polarization curves and electrochemical impedance spectroscopy were performed.

### 3.2 Results of polarization curve test

The polarization curves of API 5L X80 steel specimens exposed to 3.5 wt% NaCl, abiotic and biotic systems are shown in Figure 2.

The analysis of Figure 2 revealed that the following  $E_{\text{corr}}$  order: abiotic > 3.5 wt% NaCl > biotic. This result indicates that the steel exposed to the abiotic system presented a more positive corrosion potential, suggesting a lower aggressiveness. This behavior may be associated with the lower concentration of chloride ions in the sterile produced water ( $88.7 \times 10^{-3}$  g/L) when compared to the steel exposed to the 3.5 wt% NaCl (35 g/L) system. In addition, the presence of other species (poorly soluble salts) in the abiotic system can precipitate in the form of corrosion products, generating a protective film due to a formed physical barrier. The steel exposed to the biotic system showed to be more susceptible to corrosion. More negative potential values are associated with the action of the microorganism's metabolism such as the release of metabolites and the cathodic depolarization which intensify the corrosion process. In relation to the steel exposed to the 3.5 wt% NaCl system, the higher chloride content favored

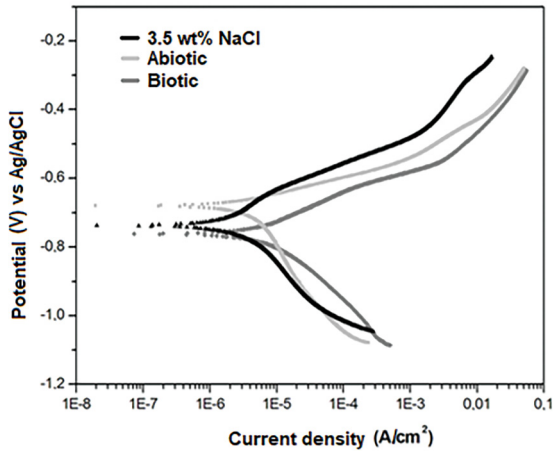


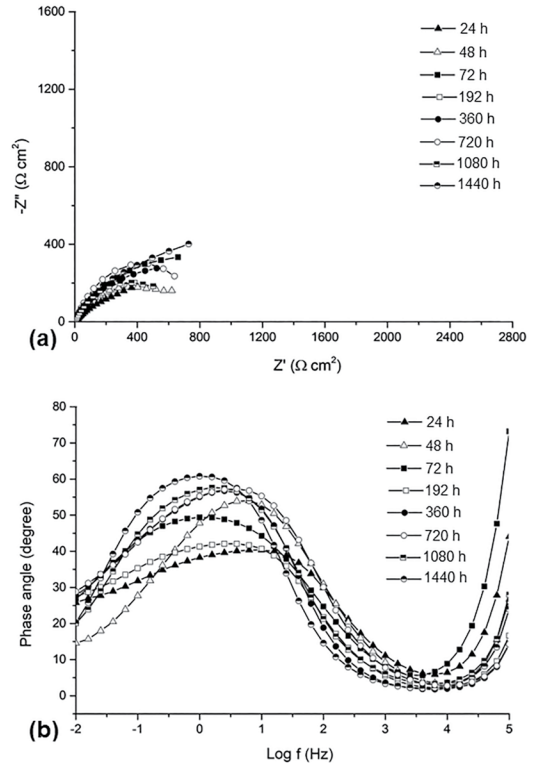
**Figure 2.** Polarization curves of API 5L X80 steel exposed to 3.5 wt% NaCl, abiotic and biotic systems.

the corrosive attack of the material, generating layers of oxides, which cannot be considered as passive because of their porosity. Although the microorganisms showed a strong influence, it was observed that the final anodic current for the abiotic and biotic systems were practically equivalent. This behavior can be attributed to the presence of sodium hypochlorite, which was used in this work with the biocidal function. Even though, this chemical compound can accelerate the corrosion of the steel<sup>20</sup>.

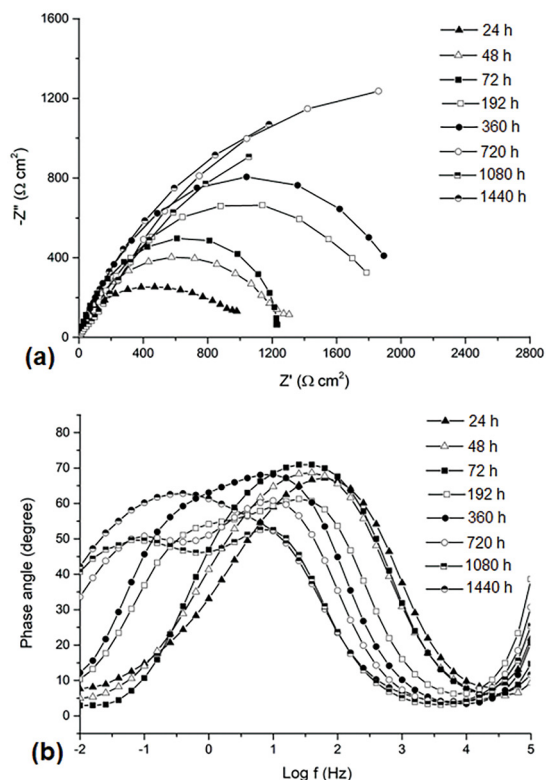
### 3.3 Results of electrochemical impedance spectroscopy test

Figure 3, 4 and 5 show the electrochemical impedance spectra of the 3.5 wt% NaCl, abiotic and biotic systems, respectively, in the first 24, 48, 72, 192, 360, 720, 1080 and 1440 hours of exposure.

The results shown in Figure 3, 4 and 5 put in evidence that the impedance spectra varied according to the exposure time in different systems. The high frequency regions of the Nyquist plot provide information about the phenomena that are occurring in the electrolyte<sup>21</sup>. In the low frequency regions of the Nyquist plot, the magnitude of the capacitive loop describes the electrochemical phenomena that are occurring at the metal/solution interface, through the anodic dissolution controlled by charge transfer processes<sup>22</sup>. Correlating the Nyquist plots for the three systems, smaller capacitive loops for the 3.5 wt% NaCl system (Figure 3 (a)) and larger for the biotic system (Figure 5 (a)) were observed. In Figure 3 (a), in the first 72 hours there was an increase of the capacitive loop, followed by a reduction with 192 hours and another increase with 720 hours. With 1080 hours, there was a decrease in the capacitive loop, and another increase with 1440 hours. The lower impedance values for the 3.5 wt% NaCl system can be attributed to the formation of non-adherent corrosion products, which when detached, allow the surface to be oxidized again, contributing to reduce the



**Figure 3.** EIS results for API 5L X80 steel in 3.5 wt% NaCl system. In (a) Nyquist plot and (b) Bode phase.



**Figure 4.** EIS results for API 5L X80 steel in abiotic system. In (a) Nyquist plot and (b) Bode phase.

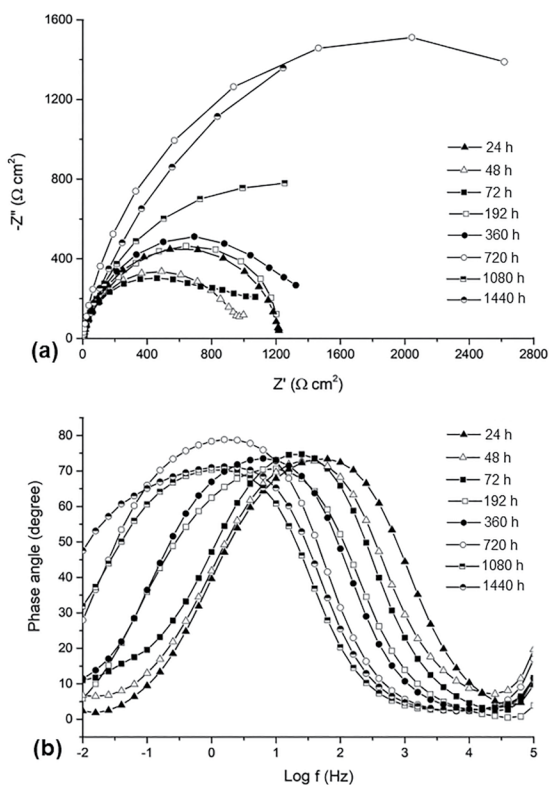


**Figure 5.** EIS results for API 5L X80 steel in biotic system. In (a) Nyquist plot and (b) Bode phase.

system impedance. Subsequently, the cycle of corrosion products is restarted, causing an increase in impedance once again. The Bode phase angle  $\theta$  vs. log frequency plot for the 3.5 wt% NaCl system (Figure 3 (b)) reveals the presence of resistive and capacitive components associated with each other, describing the phenomena that occur on the steel surface. The higher the phase angle, the greater the charge transfer resistance and consequently the corrosion reaction is more difficult. The lowest phase angle value was observed for 24 hours. During this time, the corrosion products formation was insufficient to generate a layer of protective deposits, suggesting that some areas of the metal were still exposed to the electrolyte. Higher value of phase angle was observed in the period of 1440 hours of exposure to 3.5 wt% NaCl. Possibly, corrosion products deposited on the surface after 1440 hours will be more adhered to the substrate and will have lower porosity, thus being more resistive.

The abiotic system presented intermediate capacitive loops (Figure 4 (a)), when compared to the other two systems. A continuous increase of the capacitive loop over the first 720 hours was observed. The behavior of this system may be associated with the gradual precipitation of salts from the produced water associated with corrosion products. The presence of other species besides chloride in the solution formed a less porous film which is consequently protective, creating a physical barrier to the electrolyte. AlAbbas et

al. claims that the presence of a time constant in the Bode plot phase indicates the formation of unstable corrosion products<sup>8</sup>. The Bode phase angle  $\theta$  vs. log frequency plot for the abiotic system (Figure 4 (b)) show that in the first 72 hours, in the medium frequency an unstable film was formed and evidenced by a time constant. From 192 hours onwards, two time constants were observed, signaling the formation of micropores in the film with migration to the low frequency regions. In the 3.5 wt% NaCl and abiotic systems, the electrochemical reactions at neutral pH were:

Cathodic reaction:



Anodic reaction:

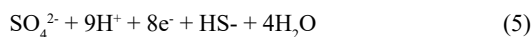


Bigger capacitive loop diameter for the steel exposed to the biotic system (Figure 5 (a)) is associated with higher system impedance values. In the first 72 hours, at low frequency, there was a gradual decrease of the capacitive loop. From the 192 to the 720 hours there was an increase of the capacitive loop with a reduction with 1080 hours and an increase with 1440 hours of exposure. The difference in resistivity over the days of exposure may be attributed to the formation of unstable biofilms and corrosion products that detach from the substrate, and subsequently reconstitute. During biofilm formation, microorganisms produce several active metabolites (organic and inorganic acids, ammonia and hydrogen sulfide) and enzymes that modify the electrochemical reactions at the metal/solution interface<sup>23-27</sup>. Associated with these factors, the oxygenation difference conditioned by the microorganisms establishes means for the creation of cells of differential aeration generating electron flow from the anode (biofilm base - less aerated area) to the cathode (top of the biofilm - more aerated area)<sup>27</sup>. After biofilm maturation, part of the structure may be detached due to enzymatic reactions with the release of microbial cells that will colonize other areas. As a consequence of this detachment, non-biofilm base metal regions are exposed and another concentration gradient is formed<sup>28</sup>. The Bode phase angle  $\theta$  vs. log frequency plot for the biotic system (Figure 5 (b)) up to the first 360 hours a peak can be observed in the medium frequency, indicating a time constant that equals a capacitive loop in the Nyquist plot (Figure 5 (a)). This single time constant indicates that the corrosion mechanism is being controlled by activation processes and attributed to the formation of unstable organic/inorganic compounds (biofilms and corrosion products)<sup>8</sup>. Figure 5 (b) shows the formation of two time constants after 720, 1080 and 1440 hours of exposure to the biotic system. The two time constants signal the formation of pores with lower porosity (micropores) in the mature biofilm, in which the phase angle peaks moved from the medium frequency

regions to the low frequency regions<sup>29</sup>. Microorganisms have different strategies to promote corrosion in metals. In the biotic system, within the group of total aerobic bacteria, the precipitating iron bacteria are the most studied. Although acid-producing anaerobic bacteria are poorly investigated, they also play an important role in the MIC mechanism. The largest representative of the group of total anaerobic bacteria is SRB, however there is also the acid-producing anaerobic bacteria<sup>10,25,30,31</sup>. This consortium of bacteria (aerobic and anaerobic) is involved according to the oxygenation gradient within the biofilm. The electrochemical mechanism of corrosion for precipitating iron bacteria can be expressed as anodic reactions to equation 2 and 3, and as cathodic reaction equation 4. The precipitating iron bacteria oxidize the ion  $Fe^{2+}$  to  $Fe^{3+}$ , having  $O_2$  as the final electron acceptor<sup>32</sup>.



The mechanism of the anodic and cathodic reactions for SRB can be expressed according to equation 2 and 5, respectively<sup>32</sup>:



Acid-producing bacteria secrete corrosive metabolites (such as volatile fatty acids) by fermentation. When these bacteria are in a medium absent from exogenous oxidants, they use a metabolite as electron acceptor to achieve redox equilibrium according to the proton reduction theory<sup>33</sup>.

The EIE results for the 3.5 wt% NaCl (Figure 3) and biotic (Figure 5) systems presented the opposite behavior to that observed in the polarization curves (Figure 2). This result is at first contradictory. With a view to explaining it, one must consider the limitations of the techniques used. The interpretation of the information generated by the electrochemical techniques should also be analyzed together. Polarization curves allow us to evaluate the type of corrosive process by imposing a potential. As it is an accelerated assay, some reactions cannot be observed due to the short exposure period. In the polarization test, the corrosion tendency can be observed and the formation of oxides may be different from those obtained in tests with a longer exposure time, resulting in different corrosion rates<sup>34</sup>. While electrochemical impedance testing is a transient technique capable of detecting electrochemical phenomena which occur at different time constants, providing information about the nature of the surface without interfering with the established corrosive process. The EIS differs from the polarization curve, which is stationary. Ergo, it only shows potential and current behavior when all physicochemical processes have had time to occur<sup>35</sup>.

To fit and analyze the EIS results, two equivalent electrochemical circuits were selected and shown in Figure 6.

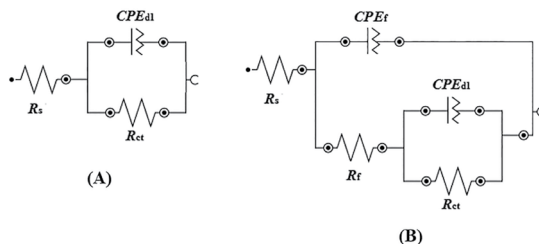


**Figure 6.** Circuits models used to fit for the EIS data (A) single layer circuit R(RC) for 3.5 wt% NaCl system and (B) double layer circuit for abiotic and biotic system R(C(R(RC))).

The electrical circuit for the 3.5 wt% NaCl system was adjusted to the Randles equivalent circuit (R(R(C))) and is shown in Figure 6 (a). In the equivalent circuit,  $R_s$  corresponds to the resistance of the solution (electrolyte),  $R_{ct}$  and  $CPE_{dl}$  represents the resistance and constant phase element (non-ideal capacitance) of the double electric layer. A circuit with two time constants of type R(C(R(RC))) was adjusted for the abiotic and biotic systems, and is shown in Figure 6 (b).  $R_f$  is the film resistance related to the ion conduction path through the pores of the film or biofilm. For the abiotic system, the circuit includes a resistance ( $R_f$ ) and a constant phase element ( $CPE_f$ ) of the oxide and salt film. For the biotic system, the equivalent circuit components  $R_f$  and  $CPE_f$  were renamed to  $R_b$  and  $CPE_b$  representing the resistance and constant phase element of the biofilm consisting of oxides, salts and microorganisms. The physical interpretation of the equivalent circuit elements for the systems was as follows: charge transfer represented by the resistors ( $R_s$ ,  $R_f$  and  $R_{ct}$ ) and dielectric surface layers represented by the non-ideal capacitor (constant phase element). When the electrolyte penetrates the film or biofilm through the pores, the dielectric constant changes. Hence, the non-ideal capacitor acquires different values according to the porosity of the film or biofilm.

Experimentally, the surface of the electrode presents heterogeneities and microimperfections (roughness), which contribute to a non-ideal behavior of the capacitor. In the equivalent electrochemical circuit (Figure 6), the capacitor element was replaced by the constant phase element (CPE), because it adjusts the conditions of deviations caused by frequency dispersion phenomena on the nonhomogeneous surface. The capacitance of the constant phase element can be estimated by the impedance of the CPE ( $Z_{CPE}$ ) expressed by equation 6<sup>32,36</sup>:

$$Z_{CPE} = Y_0^{-1} (j\omega)^{-n} \quad (6)$$

Where  $Y_0$  is the CPE parameter,  $j$  is an imaginary complex number ( $j^2 = -1$ ),  $\omega$  is the angular frequency in rad/s ( $\omega = 2\pi f$ ) and  $n$  is the deviation of the ideal behavior

for the capacitor. The parameters  $Y_0$  and  $n$  were renamed to  $Y_b$  and  $n_b$  (biofilm capacitance),  $Y_f$  and  $n_f$  (film capacitance), and  $Y_{ct}$  and  $n_{ct}$  (double layer capacitance). The values of the circuit elements for the 3.5 wt% NaCl, abiotic and biotic systems are listed in Tables 3, 4 and 5, respectively.

$R_s$  indicates the resistance of the solution between the working electrode and the reference electrode<sup>37</sup>. The values of  $R_s$  of the 3.5 wt% NaCl (Table 3), abiotic (Table 4) and biotic (Table 5) systems showed different values representing different ionic conductivities of the electrolytes throughout the time of exposure. The  $R_s$  maximum values reached in all systems with 1080 hours of exposure, this suggests that the electrolyte stabilized after the formation of the films.

In Table 3, the  $R_{ct}$  values of the API 5L X80 steel in the 3.5 wt% NaCl system increased in the first 72 hours, then it decreased with 192 hours and went up again with 720 hours. With 1080 hours these values decreased, and increased again with 1440 hours. In this system, the oscillation of the  $R_{ct}$  values with the exposure times suggests that the corrosion products formed on the surface of the steel exposed to 3.5 wt% NaCl presented more porous and less protective characteristics. In Table 4, the  $R_f$  and  $R_{ct}$  values of API 5L X80 steel in the abiotic system increased steadily over 720 hours. This behavior indicates a higher adhesion of the film consisting of precipitated salts and corrosion products on the metallic surface, being little conductive to the passage

**Table 3.** Adjusted electrochemical parameters of the EIE measurements for the 3.5 wt% NaCl system.

Time (h)	$R_s$ ( $\Omega$ cm <sup>2</sup> )	$R_{ct}$ ( $\Omega$ cm <sup>2</sup> )	$Y_{ct}$ ( $\Omega^{-1}$ cm <sup>2</sup> s <sup>-n</sup> )	$n_{ct}$
24	5.12	$1.16 \times 10^3$	$481 \times 10^{-6}$	0.435
48	6.10	$1.32 \times 10^3$	$148 \times 10^{-6}$	0.359
72	4.95	$2.61 \times 10^3$	$672 \times 10^{-6}$	0.783
192	7.21	$1.29 \times 10^3$	$4.86 \times 10^{-3}$	0.414
360	4.82	$1.44 \times 10^3$	$3.11 \times 10^{-3}$	0.432
720	1.75	$1.88 \times 10^3$	$4.22 \times 10^{-3}$	0.774
1080	9.87	$1.37 \times 10^3$	$1.49 \times 10^{-3}$	0.589
1440	3.75	$3.32 \times 10^3$	$1.68 \times 10^{-3}$	0.298

**Table 4.** Adjusted electrochemical parameters of the EIE measurements for the abiotic system.

Time (h)	$R_s$ ( $\Omega$ cm <sup>2</sup> )	$R_f$ ( $\Omega$ cm <sup>2</sup> )	$Y_f$ ( $\Omega^{-1}$ cm <sup>2</sup> s <sup>-n</sup> )	$n_f$	$R_{ct}$ ( $\Omega$ cm <sup>2</sup> )	$Y_{ct}$ ( $\Omega^{-1}$ cm <sup>2</sup> s <sup>-n</sup> )	$n_{ct}$
24	3.22	$1.96 \times 10^3$	$155 \times 10^{-6}$	0.864	$1.58 \times 10^3$	$430 \times 10^{-6}$	0.250
48	3.78	$2.47 \times 10^3$	$189 \times 10^{-6}$	0.857	$1.60 \times 10^3$	$192 \times 10^{-6}$	0.347
72	3.96	$2.79 \times 10^3$	$111 \times 10^{-6}$	0.671	$1.76 \times 10^3$	$159 \times 10^{-6}$	0.895
192	4.68	$5.15 \times 10^3$	$690 \times 10^{-6}$	0.754	$2.13 \times 10^3$	$387 \times 10^{-6}$	0.435
360	4.01	$5.51 \times 10^3$	$181 \times 10^{-6}$	0.967	$2.25 \times 10^3$	$852 \times 10^{-6}$	0.732
720	6.08	$6.08 \times 10^3$	$794 \times 10^{-6}$	0.837	$3.39 \times 10^3$	$1.84 \times 10^{-3}$	0.741
1080	7.67	$5.63 \times 10^3$	$1.15 \times 10^{-3}$	0.824	$3.19 \times 10^3$	$3.14 \times 10^{-3}$	0.685
1440	4.06	$6.19 \times 10^3$	$3.58 \times 10^{-3}$	0.725	$4.57 \times 10^3$	$4.59 \times 10^{-3}$	0.812

**Table 5.** Adjusted electrochemical parameters of the EIE measurements for the biotic system.

Time (h)	$R_s$ ( $\Omega$ cm <sup>2</sup> )	$R_b$ ( $\Omega$ cm <sup>2</sup> )	$Y_b$ ( $\Omega^{-1}$ cm <sup>2</sup> s <sup>-n</sup> )	$n_b$	$R_{ct}$ ( $\Omega$ cm <sup>2</sup> )	$Y_{ct}$ ( $\Omega^{-1}$ cm <sup>2</sup> s <sup>-n</sup> )	$n_{ct}$
24	1.88	$3.97 \times 10^3$	$282 \times 10^{-6}$	0.871	$3.05 \times 10^3$	$695 \times 10^{-6}$	0.811
48	2.67	$2.54 \times 10^3$	$260 \times 10^{-6}$	0.873	$2.81 \times 10^3$	$2.45 \times 10^{-3}$	0.374
72	2.42	$2.19 \times 10^3$	$340 \times 10^{-6}$	0.905	$2.63 \times 10^3$	$2.73 \times 10^{-3}$	0.462
192	2.46	$4.27 \times 10^3$	$370 \times 10^{-6}$	0.933	$3.17 \times 10^3$	$742 \times 10^{-6}$	0.705
360	2.56	$4.91 \times 10^3$	$928 \times 10^{-6}$	0.879	$3.31 \times 10^3$	$1.02 \times 10^{-3}$	0.243
720	2.41	$7.62 \times 10^3$	$1.60 \times 10^{-3}$	0.915	$6.34 \times 10^3$	$1.52 \times 10^{-3}$	0.719
1080	3.23	$6.27 \times 10^3$	$3.15 \times 10^{-3}$	0.831	$4.08 \times 10^3$	$2.44 \times 10^{-3}$	0.748
1440	2.22	$7.11 \times 10^3$	$2.15 \times 10^{-3}$	0.908	$6.12 \times 10^3$	$1.56 \times 10^{-3}$	0.597

of the electric current. After 1080 hours,  $R_f$  and  $R_{ct}$  values decreased indicating the detachment of parts of the surface film. The steel areas exposed to the electrolyte started to oxidize again and the deposition of corrosion products occurred, which act as a barrier on the surface, observed by an increase in  $R_f$  and  $R_{ct}$  after 1440 hours. In Table 5 there was a decrease in  $R_b$  and  $R_{ct}$  values in the first 72 hours of exposure of the API 5L X80 steel to the biotic system. This behavior means loss or displacement of parts of the biofilm initially formed, exposing the metal surface to the corrosive species present in the solution, denoting the instability of this biofilm. From the 192 to the 720 hours, the  $R_b$  and  $R_{ct}$  values increased, indicating that the microorganisms colonized the steel surface forming the biofilm associated with the corrosion products. However, the presence of the microorganisms favors pitting corrosion, accompanied by damage to the protective properties of the biofilm, inducing an increase in the active surface area of the steel<sup>29</sup>. With 1080 hours, the  $R_b$  and  $R_{ct}$  values decreased indicating that the biofilm presented micropores that favored the diffusion of the electrolyte to the metallic surface. Subsequently, these values increased with 1440 hours indicating biofilm restructuring. The variation of the  $R_{ct}$  values was consistent with the impedance arcs in the Nyquist plot (Figure 5 (a)). High capacitance values indicate that the film (corrosion products with microorganisms and/or precipitated salts) has a high electrical conductivity, due to the higher porosity and consequently greater area of contact between film and electrolyte<sup>38,39</sup>. For the biotic system, the highest values of  $Y_b$  were at 720, 1080 and 1440 hours suggesting that there was an increase in biofilm porosity. The formation of the biofilm at the interface causes instability in the capacitance due to the phases of microbiological growth associated with the increase of active regions through the pores formed in the biofilm<sup>29</sup>. The capacitance variation was observed in other biological systems already studied<sup>22,40,41</sup>. Values of  $n$  near 1 suggest more surface homogeneity and the smaller this

value is, the more heterogeneous will be the surface, due to the greater roughness<sup>42</sup>. In all systems studied, a decrease in the value of  $n$  ( $n < 1$ ) could be observed, signaling the non-ideal behavior of the capacitor due to the dispersing effect of the frequencies. For the abiotic system, the values of  $n_f$  were in the range between 0.671 and 0.967, indicating that the system alternated between a heterogeneous and homogeneous surface. While in the biotic system, the values of  $n_b$  oscillated between 0.831 and 0.933, denoting an almost homogeneous surface.

### 3.4 Analysis of films and corrosion morphology

For better understanding of the corrosion process, it was necessary to evaluate the structure of the film (Figure 7) and the corrosion morphology (Figure 8) formed on the surface of API 5L X80 steel after 15 days of exposure to 3.5 wt% NaCl, abiotic and biotic systems.

Figure 7 shows the different morphologies and arrangements of the films on the surface of the coupons studied. Figure 7 (a) of the 3.5 wt% NaCl system shows the compact corrosion products on which the crystals of sodium chloride are adhered. The morphology of the film formed on the surface exposed to the abiotic system (Figure 7 (b)) was covered by crystals of salts and the absence of microbial cells confirmed the sterility of this system. A very common problem in the petroleum industry is the corrosion of carbon steel by the presence of salts and solids dissolved in the produced water<sup>1</sup>. The minerals present in the produced water are due to the super saturation of inorganic salts (carbonate, sulphate, sulphide salts (calcium, barium, strontium and iron) and sodium chloride), which can cause reduction of flow, water carrying capacity, as well as a total obstruction of the pipeline<sup>43</sup>. Figure 7 (c) shows the adhesion of the microbial consortium on the steel surface, more specifically of bacterial cells (rods) aggregated by extracellular polymer substance and a significant amount of corrosion products forming the biofilm matrix. Precipitating

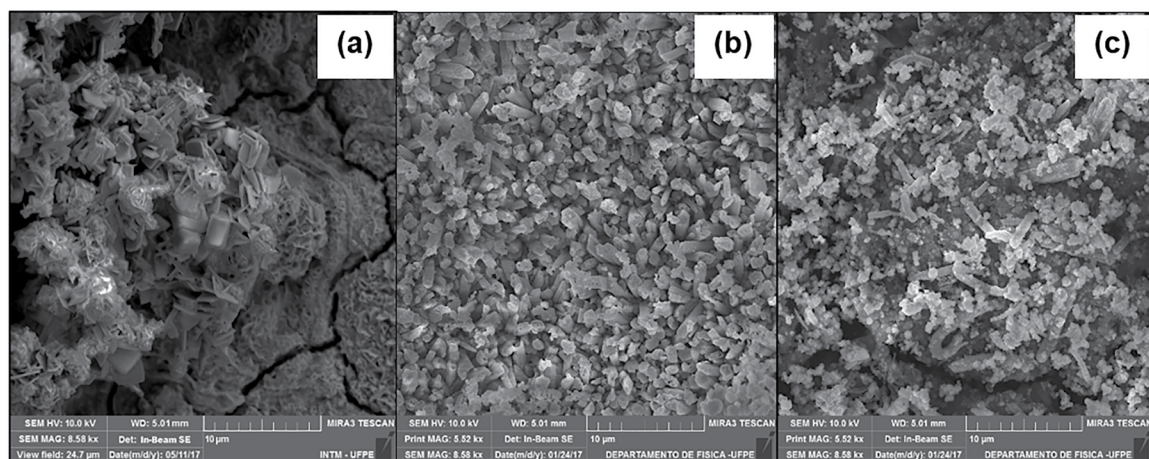


**Figure 7.** Micrographs of the films formed on the surface of API 5L X80 steel coupons after 15 days of exposure to the (a) 3.5 wt% NaCl, (b) abiotic and (c) biotic systems.

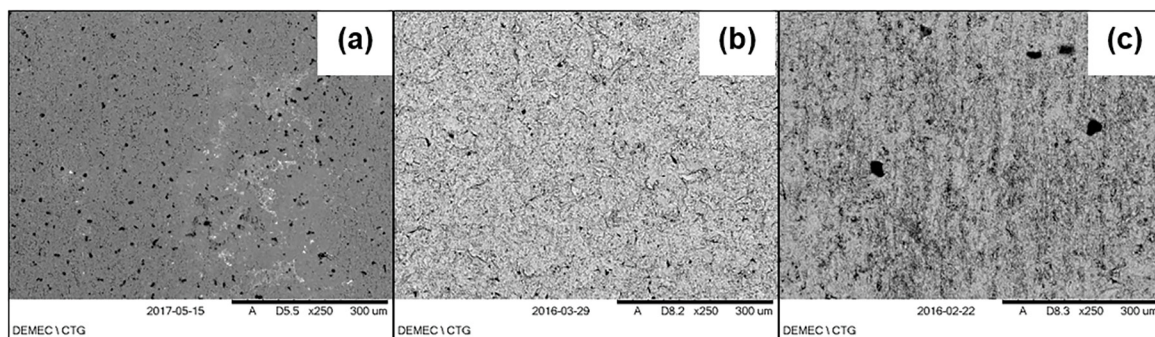


**Figure 8.** Micrographs of the surface of the API 5L X80 steel coupons after the removal of the films in the (a) 3.5 wt% NaCl, (b) abiotic and (c) biotic systems.

iron bacteria and SRB form biofilms containing agglomerates of exopolysaccharides that facilitate colonization of metal surfaces. Within the biofilm, precipitating iron bacteria produce precipitates of iron oxides<sup>40,44</sup>. After removal of the films and acid pickling, a high density of pits with a small diameter on the surface of the steel exposed to 3.5 wt% NaCl was observed in Figure 8 (a). Figure 8 (b) showed minimal corrosion damage with almost imperceptible pits in the steel exposed to the abiotic system. The coupon exposed to the biotic system (Figure 8 (c)) exhibited a surface with pitting corrosion presenting larger diameter bumps and smaller amounts when compared to Figure 8 (a). The formation of the biofilm established favorable conditions to the metabolic activity of the consortium of microorganisms that induced the formation of corrosive pits in the steel. Precipitating iron bacteria and SRB can cause pitting corrosion after the formation of biofilms<sup>32</sup>. Another important group are the acid-producing bacteria that promote the electrochemical oxidation of metals by secreted acids. The action of these bacteria is intensified when these metabolites adhere to the metal/solution interface<sup>45</sup>. The interaction between these bacteria present in the produced water (Table 2) and the steel may have contributed to the initial formation of pits.

#### 4. Conclusions

The microbiological corrosion of API 5L X80 steel in produced water was studied through electrochemical tests and surface analysis. A system with 3.5 wt% NaCl solution was also adopted for comparison purposes. The corrosion potential measured as a function of time showed that steel presented a higher tendency to corrosion in the following order: 3.5 wt% NaCl < abiotic < biotic. The polarization curve tests revealed the effect of the microorganisms in the biotic system by displacing the potential to more cathodic values and increasing the corrosion current density in relation to the other two systems. The metabolic activity of the microorganism consortium resulted in increased anodic dissolution of the steel. The EIS results indicated that the oxides formed on the steel in the 3.5 wt% NaCl system presented high porosity promoting the permeation

of the electrolyte to the surface, promoting high density of pits. For steel in the abiotic system, the properties of the film with lower porosity confer intermediate protection among the investigated systems, causing less aggressive pitting corrosion. In the biotic system, the electrochemical phenomenon in the metal/solution interface was modified by the formation, detachment and corrosive factors of the biofilm. The formation of corrosion pits with larger diameter was attributed to microbiological activity. The choice of the Randles equivalent electrochemical circuit (R(RC)) for the 3.5 wt% NaCl system and the R(C(R(RC))) circuit for the abiotic and biotic systems allowed to consistently adjust the impedance data. Microbiological corrosion is a predicted problem in the oil and natural gas industry, which needs to be studied constantly given the increasing use of API 5L X80 steel in pipelines.

#### 5. Acknowledgements

The authors thank Programa de Recursos Humanos da Petrobras - PRH 203, ANP and Finep for financial support in the development of this work. To the Department of Physics of the UFPE and to the INTM for the concession of the analysis in the SEM.

#### 6. References

1. Deyab MA, El Bali B, Essehli R, Ouarsal R, Lachkar M, Fuess H.  $\text{NaNi}(\text{H}_2\text{PO}_3)_3 \cdot \text{H}_2\text{O}$  as a novel corrosion inhibitor for X70-steel in saline produced water. *Journal of Molecular Liquids*. 2016;216:636-640.
2. Jain P, Sharma M, Dureja P, Sarma PM, Lal B. Bioelectrochemical approaches for removal of sulfate, hydrocarbon and salinity from produced water. *Chemosphere*. 2017;166:96-108.
3. Al-Haleem AA, Abdulah HH, Saeed EAJ. Components and treatments of oilfield produced water. *Al-Khwarizmi Engineering Journal*. 2010;6(1):24-30.
4. Araújo L, Carvalho L, Reznik L, Lutterbach M, Sérvulo E. Efeito de biocidas na corrosão induzida microbiologicamente do aço duplex em água de produção de petróleo. *Corrosão e Protecção dos Materiais*. 2013;32(4):108-114.

5. Albuquerque AC, Andrade C, Neves B. Biocorrosão: da integridade do biofilme à integridade do material. *Corrosão e Proteção dos Materiais*. 2014;33(1-2):18-23.
6. Ossai CI, Boswell B, Davies IJ. Pipeline failures in corrosive environments – A conceptual analysis of trends and effects. *Engineering Failure Analysis*. 2015;53:36-58.
7. Videla HA, Herrera LK. Microbiologically influenced corrosion: looking to the future. *International Microbiology*. 2005;8(3):169-180.
8. Al-Abbas FM, Williamson C, Bhola SM, Spear JR, Olson DL, Mishra B, et al. Influence of sulfate reducing bacterial biofilm on corrosion behavior of low-alloy, high-strength steel (API-5L X80). *International Biodeterioration and Biodegradation*. 2013;78:34-42.
9. Mishra B. Corrosion characterization of advanced steels for use in the oil & gas industry. *International Journal of Metallurgical Engineering*. 2013;2(2):221-229.
10. Liu HW, Chen B, Zhang F, Qin S, Zhang GA, Liu HF. Effects of iron-oxidizing bacteria on carbon steel in oilfield produced water. *ECS Transactions*. 2014;59(1):409-420.
11. Wu T, Xu J, Yan M, Sun C, Yu C, Ke W. Synergistic effect of sulfate-reducing bacteria and elastic stress on corrosion of X80 steel in soil solution. *Corrosion Science*. 2014;83:38-47.
12. Wu T, Xu J, Sun C, Yan M, Yu C, Ke W. Microbiological corrosion of pipeline steel under yield stress in soil environment. *Corrosion Science*. 2014;88:291-305.
13. Wu T, Yan M, Zeng D, Xu J, Sun C, Yu C, et al. Hydrogen permeation of X80 steel with superficial stress in the presence of sulfate-reducing bacteria. *Corrosion Science*. 2015;91:86-94.
14. American Public Health Association (APHA), American Water Works Association, Water Environment Federation. *Standard methods for the examination of water and wastewater*. Washington, DC: Centennial Edition; 2012.
15. Oliveira ESD, Pereira RFC, Melo IR, Lima MAGA, Urtiga Filho SL. Corrosion behavior of API 5L X80 steel in the produced water of onshore oil recovery facilities. *Materials Research*. 2017;20(Suppl 2):432-439.
16. Postgate JR. *The sulphate-reducing bacteria*. 2<sup>nd</sup> ed. New York: Cambridge University Press; 1984.
17. Companhia Ambiental do Estado de São Paulo (CETESB). *Norma L5.201 – Contagem de bactérias heterotróficas – Método de ensaio*. São Paulo (SP): CETESB; 2006.
18. American Society for Testing and Materials (ASTM). *ASTM G1-03 – Standard practice for preparing, cleaning, and evaluating corrosion test specimens*. West Conshohocken, PA: ASTM International; 2011.
19. Liu Y, Zhang Y, Yuan J. Influence of produced water with high salinity and corrosion inhibitors on the corrosion of water injection pipe in Tuha oil field. *Engineering Failure Analysis*. 2014;45:225-233.
20. Oliveira SH, Lima MAGA, França FP, Vieira MRS, Silva P, Urtiga Filho SL. Control of microbiological corrosion on carbon steel with sodiumhypochlorite and biopolymer. *International Journal of Biological Macromolecules*. 2016;88:27-35.
21. Carvalho LA, Andrade AR, Bueno PR. Espectroscopia de impedância eletroquímica aplicada ao estudo das reações heterogêneas em ânodos dimensionalmente estáveis. *Química Nova*. 2006;29(4):796-804.
22. Castaneda H, Benetton XD. SRB-Biofilm influence in active corrosion sites formed at the steel-electrolyte interface when exposed to artificial seawater conditions. *Corrosion Science*. 2008;50:1169-1183.
23. Sutherland IW. The biofilm matrix – an immobilized but dynamic microbial environment. *Trends in Microbiology*. 2001;9(5):222-227.
24. Beech IB, Sunner J. Biocorrosion: towards understanding interactions between biofilms and metals. *Current Opinion in Biotechnology*. 2004;15(3):181-186.
25. Al-Abbas FM, Bhola R, Spear JR, Olson DL, Mishra B. Electrochemical characterization of microbiologically influenced corrosion on linepipe steel exposed to facultative anaerobic *Desulfovibrio sp.* *International Journal of Electrochemical Science*. 2013;8:859-871.
26. Karn SK, Duan J. Perspective on microbial influenced corrosion. *Journal of Cleaner Production*. 2017;141:180-181.
27. Beech IB, Gaylarde CC. Recent advances in the study of biocorrosion: an overview. *Revista de Microbiologia*. 1999;30:177-190.
28. Gentil V. *Corrosão*. 6<sup>a</sup> ed. Rio de Janeiro: LTC - Livros Técnicos e Científicos S.A.; 2011.
29. Belkaid S, Ladjouzi MA, Hamdani S. Effect of biofilm on naval steel corrosion in natural seawater. *Journal of Solid State Electrochemistry*. 2011;15:525-537.
30. Emerson D, Fleming EJ, McBeth JM. Iron-oxidizing bacteria: an environmental and genomic perspective. *Annual Reviews Microbiology*. 2010;64:561-583.
31. Zarasvand KA, Rai VR. Microorganisms: induction and inhibition of corrosion in metals. *International Biodeterioration and Biodegradation*. 2014;87:66-74.
32. Liu H, Fu C, Gu T, Zhang G, Lv Y, Wang H, et al. Corrosion behavior of carbon steel in the presence of sulfate reducing bacteria and iron oxidizing bacteria cultured in oilfield produced water. *Corrosion Science*. 2015;100:484-495.
33. Xu D, Li Y, Gu T. Mechanistic modeling of biocorrosion caused by biofilms of sulfate reducing bacteria and acid producing bacteria. *Bioelectrochemistry*. 2016;110:52-58.
34. Pereira RFC, Oliveira ESD, Lima MAGA, Brasil SLDC. Corrosion of galvanized steel under different soil moisture contents. *Materials Research*. 2015;18(3):563-568.
35. Bastos IN. As sofisticadas armas do combate à corrosão. *Corrosão e Proteção*. 2016;13(61):3-34.
36. Ituen E, Akaranta O, James A. Green anticorrosive oilfield chemicals from 5-hydroxytryptophan and synergistic additives for X80 steel surface protection in acidic well treatment fluids. *Journal of Molecular Liquids*. 2016;224:408-419.
37. Zhang H, Tian Y, Wan J, Zhao P. Study of biofilm influenced corrosion on cast iron pipes in reclaimed water. *Applied Surface Science*. 2015;357:236-247.

38. Öskan S, Hapçı G, Orhan G, Kazmanlı K. Electrodeposited Ni/SiC nanocomposite coatings and evaluation of wear and corrosion properties. *Surface and Coatings Technology*. 2013;232:734-741.
39. Duan J, Wu S, Zhang X, Huang G, Du M, Hou B. Corrosion of carbon steel influenced by anaerobic biofilm in natural seawater. *Electrochimica Acta*. 2008;54:22-28.
40. Cetin D, Aksu ML. Corrosion behavior of low-alloy steel in the presence of *Desulfotomaculum* sp. *Corrosion Science*. 2009;51(8):1584-1588.
41. Chen X, Wang G, Gao F, Wang Y, He C. Effects of sulphate-reducing bacteria on crevice corrosion in X70 pipeline steel under disbonded coatings. *Corrosion Science*. 2015;101:1-11.
42. Dong ZH, Shi W, Ruan HM, Zhang GA. Heterogeneous corrosion of mild steel under SRB-biofilm characterised by electrochemical mapping technique. *Corrosion Science*. 2011;53(9):2978-29.
43. Liu Y, Kan A, Zhang Z, Yan C, Yan F, Zhang F, et al. An assay method to determine mineral scale inhibitor efficiency in produced water. *Journal of Petroleum Science and Engineering*. 2016;143:103-112.
44. Liu H, Gu T, Zhang G, Wang W, Dong S, Cheng Y, et al. Corrosion inhibition of carbon steel in CO<sub>2</sub>-containing oilfield produced water in the presence of iron-oxidizing bacteria and inhibitors. *Corrosion Science*. 2016;105:149-160.
45. Little BJ, Lee JS. *Microbiologically influenced corrosion*. New Jersey: R. Winston Revie Series; 2007.